

Microwave assistant production of a high performance adsorbent from rice husk

Hadis Bashiri[†], Samira Nesari, and Malihe Sarabadan

Department of Physical Chemistry, Faculty of Chemistry, University of Kashan, Kashan, Iran

(Received 11 August 2019 • accepted 1 December 2019)

Abstract—Microwave radiation was used for synthesis of an adsorbent using rice husk. The activation of the rice husk sample was performed by H_3PO_4 and 6 min of the microwave radiation with power 700 W. The synthesized adsorbent was characterized by SEM, FT-IR, BET and XRD techniques. These analyses showed the prepared adsorbent is an amorphous and mesoporous nano-adsorbent with BET surface area $276.43\text{ m}^2/\text{g}$. It has some aromatic groups and O-H, C=C, C-O and C=O bands in its structure. Adsorption of alizarin yellow on the synthesized nano-adsorbent was investigated and the influences of adsorbent dosage (0.1-2 g/L) and temperature (25-40 °C) on dye removal from aqueous solution were investigated. The kinetic, equilibrium and thermodynamics studies of alizarin yellow removal from aqueous solution using the prepared adsorbent were carried out. The adsorption performance of alizarin yellow on the prepared adsorbent was compared with a commercial activated carbon. The importance of this study is in providing a condition for preparation of a low cost adsorbent with high adsorption capacity (712.63 mg/g) for alizarin yellow. The comparison of adsorption capacities of the prepared adsorbent from rice husk and other adsorbents proved it is a perfect adsorbent.

Keywords: Adsorption, Dye Removal, Kinetic, Alizarin Yellow, Equilibrium, Microwave, Rice Husk, Activated Carbon, Adsorption Capacity, Wastewater Treatment, Thermodynamics

INTRODUCTION

Reduction of pollutants, especially dyes, from wastewater of some industries such as plastics, papers and textiles is necessary. Some dyes are toxic, carcinogenic and very hazardous. Uğurlu et al. [42] maintained that the frequent exposure to some dyes may create injury to the eyes and skin of humans and animals. Parra et al. [27] mentioned that alizarin yellow is an anionic dye with some toxic effects. It is used in various industries and textiles and is a stable dye that cannot be absolutely degraded by different methods. Its resistance to degradation is related to its complex structure and it can cause many biological problems for human and animal health.

The object of dye removal from aqueous solution is the important purpose of many researchers. To this purpose, many techniques have been investigated. An easy and economic method for dye removal from aqueous solution is adsorption by low cost and available adsorbents, such as zeolites [33], montmorillonite [32] and activated carbons [2,9]. With modification of agricultural wastes to activated carbon, high adsorption capacity can be obtained. Activated carbons have advantages like large surface area, durability, various structures and also ability to change the porous structures [19]. Activated carbons can be obtained from agricultural materials [46] such as olive stone [42], almond shells [40], date stone [13], orange peel [36] and rice husk [25,26,38].

The world rice husk is estimated at about 100 million tons per year and it remains as an unused waste material [37]. Rice husk is low cost, available, abundant everywhere and it is rich in carbon. A large number of possible industrial applications of rice husk can

be investigated and also, it can be an excellent choice for preparation of activated carbon. Many researchers have utilized some different methods to prepare activated carbon from rice husk. Zhang et al. [45] prepared activated carbon by pyrolysis and activation steam of rice husk for removal of Cu(II) from aqueous solution. Menya et al. [25] used the rice husk to prepare activated carbon by chemical activation using H_3PO_4 or KOH as the activating agents. Chen et al. [8] employed sulfuric acid-assisted carbonization and H_3PO_4 activation to convert NaOH pre-treated rice husk to an activated carbon for methylene blue removal. Gupta et al. [12] employed hydrogen peroxide activation to prepare the activated carbon for removal of Safranin-T. Hsu and Pan [16] studied adsorption of paraquat using a methacrylic acid (MAA)-modified rice husk. Lin et al. [23] prepared activated carbon from the NaOH pre-treated rice husk.

Preparation of the activated carbons by microwave radiation is a novel method. Microwave energy can induce dipole rotation on the carbon atoms for 2,450 million times per second and it causes a strong friction between the molecules which creates heat energy within the material [24]. As Ji et al. [18] wrote, the advantages of this method are the high heating rate, shorter used time and small equipment size. Sharif et al. [34] used microwave heating to prepare activated carbon from sesame seed shells using $ZnCl_2$ activation. Recently, activated carbons with high surface areas have been prepared from sunflower seed husk [5], pistachio shells [6] and almond shells [17] with both microwave and conventional heating assisted $ZnCl_2$ activation. Hejazifar et al. [14] used microwave irradiation on grapevine rhytidome to prepare granular activated carbon for methyl violet removal from aqueous solution. They found the optimum condition for adsorbent preparation was H_3PO_4 concentration 85%, acid/precursor weight ratio 5 : 1, impregnation time 24 h, microwave power 400 W, microwave radiation time 2 min,

[†]To whom correspondence should be addressed.

E-mail: hbashiri@kashanu.ac.ir, h.bashiri@ymail.com

Copyright by The Korean Institute of Chemical Engineers.

oven temperature 110 °C and oven heating time of 7 h.

The aim of this study was the microwave assisted preparation of a low cost adsorbent from rice husk (AD-RH) with high adsorption capacity for alizarin yellow. We tried the obtained optimum condition by Hejazifar et al. to prepare an adsorbent from rice husk, but the obtained adsorbent did not have high adsorption capacity (59.20 mg/g) [4]. Therefore, in this study, the same condition has been used with microwave power 700 W and microwave radiation time 6 min. The other purpose of this study was to investigate the influences of adsorbent dosage and temperature on dye removal percentage. Characterization of prepared adsorbent was done by measuring XRD, BET, SEM and FT-IR analysis. The kinetic, equilibrium and thermodynamics of alizarin yellow removal on the AD-RH were studied. The adsorption capacity of AD-RH for alizarin yellow was compared with the commercial activated carbon of Merck company (CAC) and some other adsorbents.

EXPERIMENTAL

1. Materials and Methods

Rice husk was obtained from a local farmer in the north of Iran (Ramsar city). Alizarin yellow was obtained from Merck (Germany); the chemical structure of alizarin yellow is shown in Fig. 1. Phosphoric acid and CAC were obtained from Merck. Deionized water was used to prepare the dye solutions. Different concentrations of CV solutions were prepared by further dilution from the stock solution of 1,000 mg/L. Dye concentrations of the solutions were determined using a UV-vis spectrophotometer (PG Instrument LTD Model T70). Batch adsorption experiments were performed in 100 mL conical flasks in a temperature-controlled water bath shaker (N-bioteck).

SEM model Hitachi S-4160 Japan was used to study the gold-coated samples. FT-IR Magna 550-Nicolet was applied to determine the functional groups of adsorbent, and it was performed in the range of 400-4,000 cm^{-1} . X-ray diffraction (XRD, Philips X'pert Pro MPD) was performed to characterize the phase and structure of the prepared adsorbent using $\text{Cu K}\alpha$ radiation (40 KV and 40 mA). Microwave oven model GE280/GE281 was used for radiation on the rice husk. The specific surface area was determined using surface area analyzer (Belsorb Gas Adsorption Analyzer).

2. Preparation of an Adsorbent from Rice Husk (AD-RH)

The rice husks sample was washed with deionized water for several times to remove the adhering soil and dust. Then, it was dried at 70 °C overnight and mixed with phosphoric acid (85 wt%) in the mass ratio 1 : 5 (rice husk to phosphoric acid). The mixture was placed in a microwave oven for 6 min with power 700 W. Then,

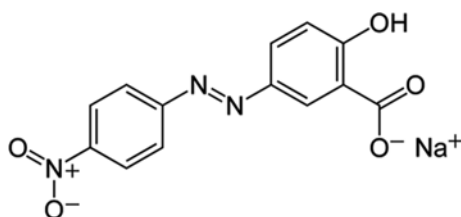


Fig. 1. Chemical structure of alizarin yellow.

the sample was placed in an oven at 110 °C for 7 h. The obtained solid product was washed with hot (95 °C) and cold (20 °C) deionized water until the natural pH was obtained. The sample was dried in an oven 50 °C overnight.

3. Adsorption Procedure

3-1. Adsorption Equilibrium Procedure

Batch experiments for the adsorption equilibrium studies were performed in a 100 mL conical flask by mixing 30 mL of the alizarin yellow dye solution with 0.03 g of the adsorbent. The mixture was placed at 25 °C, at constant speed of 200 rpm with contact time 48 h, with initial dye concentrations 6, 10, 30, 40 and 45 mg/L. When the system reached equilibrium, the mixtures were filtered. The residual dye concentrations in solutions were determined using a UV-Visible spectrophotometer at the maximum adsorption wavelength (532.5 nm) of alizarin yellow. The amount of the adsorbed dye on the surface at equilibrium, q_e (mg/g), was calculated using Eq. (1):

$$q_e = \frac{(C_0 - C_e)V}{W} \quad (1)$$

where C_0 and C_e (mg/L) are the concentrations of alizarin yellow at the start of adsorption and at equilibrium, respectively. W shows the mass of the used adsorbent (g) and V is the volume of the solution (L).

The removal efficiency of alizarin yellow dye, R (%), was determined using Eq. (2):

$$R\% = \frac{C_0 - C_e}{C_0} \times 100 \quad (2)$$

3-2. Adsorption Kinetics Procedure

Adsorption kinetics was performed by batch technique. In 100 mL-stoppered Erlenmeyer flasks, 0.03 g of the adsorbent was added to 30 mL of dye solution (6, 8 and 10 mg/L). The flasks were placed in the shaker at 200 rpm and 25 °C. The amount of adsorbed dye at each time, q_t (mg/g), was obtained using Eq. (3):

$$q_t = \frac{(C_0 - C_t)V}{W} \quad (3)$$

where C_t (mg/L) is the concentration of alizarin yellow dye at each time.

RESULTS AND DISCUSSION

1. Characterization of Adsorption

The morphology and surface chemistry of the prepared adsorbent were characterized using FT-IR, XRD, SEM and BET analysis.

1-1. FT-IR Spectrum

The Fourier-transform infrared spectra for the untreated rice husk and AD-RH are shown in Fig. 2. The FT-IR spectra for the untreated rice husks and the AD-RH are almost similar. The spectrum of the rice husks sample has six peaks at around 3,430, 2,923, 1,637, 1,384, 1,110 and 669 cm^{-1} and the spectrum of the AD-RH sample has six peaks at around 3,430, 1,629, 1,384, 1,169, 677 and 493 cm^{-1} . The spectra of the samples show a peak at about 3,430 cm^{-1} , assigned to the stretching vibration of intra and intermolec-

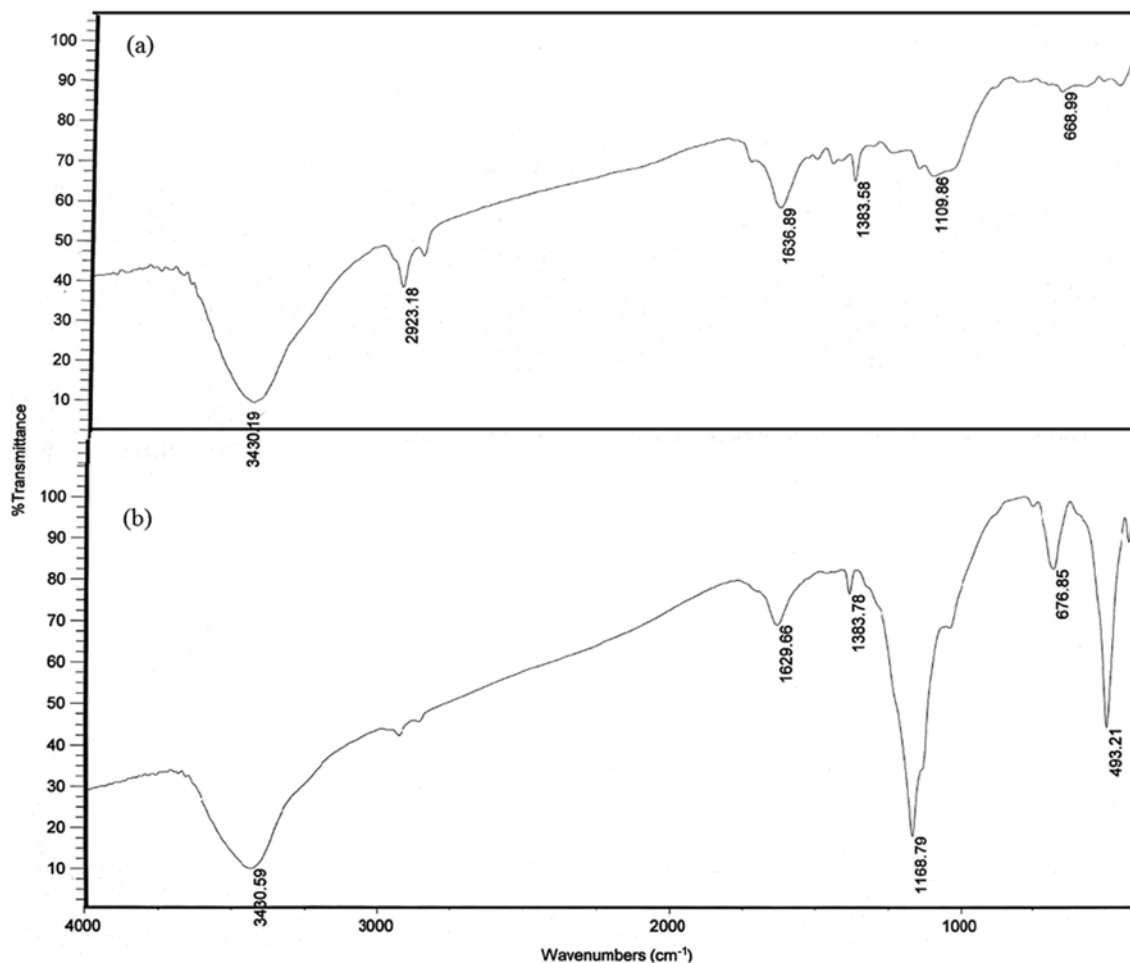


Fig. 2. FT-IR spectra of (a) the rice husks sample and (b) the AD-RH sample.

ular hydroxyl groups (-OH). The peaks for samples at about 1,384 and 2,923 cm^{-1} are attributed to the C-H stretching vibration of methyl and methylene groups. The decrease in the intensity of the peak at 2,923 cm^{-1} in the spectrum of the AD-RH sample is probably due to the decrease in CH groups on the surface of the prepared activated carbon. The bands seen at about 1,630 cm^{-1} may be related to the aromatic ring or C=C stretching vibration in the samples. The peaks at 1,110 and 1,169 cm^{-1} are usually found with oxidized carbons and have been assigned to C-O stretching vibration in the ester group. The increase in the intensity of the peak at 1,169 cm^{-1} in the spectrum of the AD-RH sample indicates the number of oxygen-containing functional groups in this sample has increased. The bands at 669 and 677 cm^{-1} could be related to C=O asymmetric vibration. In addition, the peak in the FTIR diagram of AD-RH sample appearing at 493 cm^{-1} is due to bending vibrations of the phosphorus and oxygen bonds, which shows the presence of phosphorus in the AD-RH sample. Some functional groups in the activated samples can be beneficial for the adsorption process.

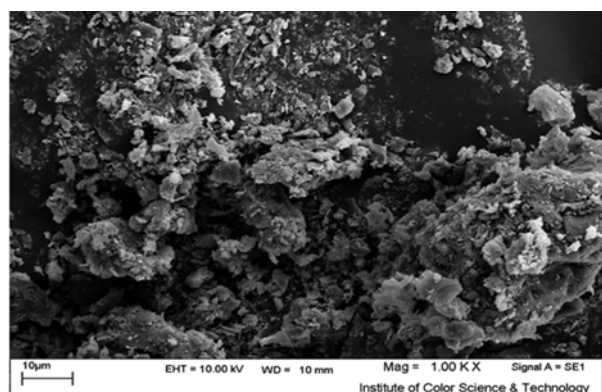
1-2. SEM

Scanning electron microscopy is a suitable method to study the surface morphology and the particles size of adsorbent. Fig. 3 shows SEM micrograph of AD-RH produced at three different

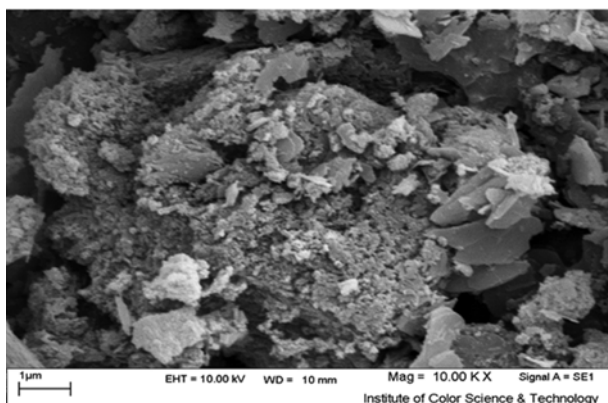
magnifications. The SEM images show the AD-RH sample has well-developed pore structures with caves, uneven and rough surface morphology. It has a clear irregular porous structure with different sizes. Because of the large and well-developed pores clearly found on the surface of the AD-RH, there are various possibilities for trapping of alizarin yellow molecules into pores. Fig. 3(c) shows particle size of AD-RH in the nanometer range and it can be a highly efficient nano-adsorbent.

1-3. XRD

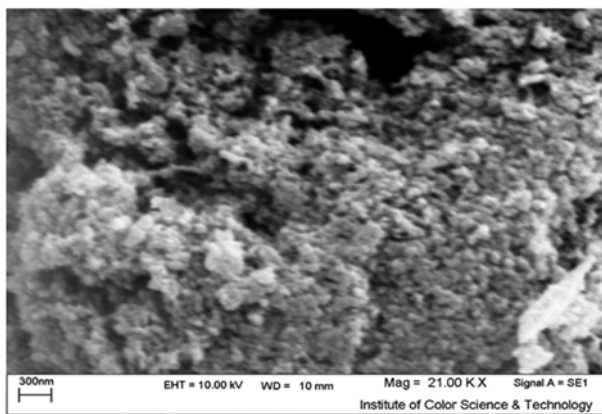
Fig. 4 illustrates the X-ray diffraction (XRD) pattern of (a) the rice husks sample and (b) the AD-RH sample. Fig. 4(a) shows the XRD pattern of the rice husks sample, and the broad peak indicates it is amorphous in nature. Fig. 4(b) shows the XRD pattern of the AD-RH sample and appearance of broad diffraction background, and the absence of sharp peaks indicates it is a largely amorphous structure. There are two broad diffraction backgrounds at around 20-30° and 40-50° in the spectrum of AD-RH sample. The appearance of a broad peak between 20-30° in the XRD pattern of the rice husks sample as well as in the activated carbon indicates the presence of carbon. The intensity peak at around $2\theta \approx 25^\circ$ indicates the samples contain graphite, and the appearance of this peak in the XRD pattern of AD-RH sample signifies an increasing regularity of crystalline structure, which will result in a better layer



(a)



(b)



(c)

Fig. 3. SEM images of AD-RH (a) magnification 100, (b) magnification 1000, (c) magnification 2100.

alignment. The XRD of the AD-RH sample shows another hump at 2θ range $40-50^\circ$, which means it is more highly disordered than the unmodified one.

1-4. N_2 Adsorption-desorption Isotherms

The N_2 adsorption-desorption isotherms of the rice husk and AD-RH samples are shown in Fig. 5. The N_2 adsorption-desorption isotherm of the rice husk sample is typical of microporous material, and this isotherm for the AD-RH sample is typical of mesoporous material. The specific surface area, total pore volume and mean pore diameter of the rice husk and AD-RH samples obtained

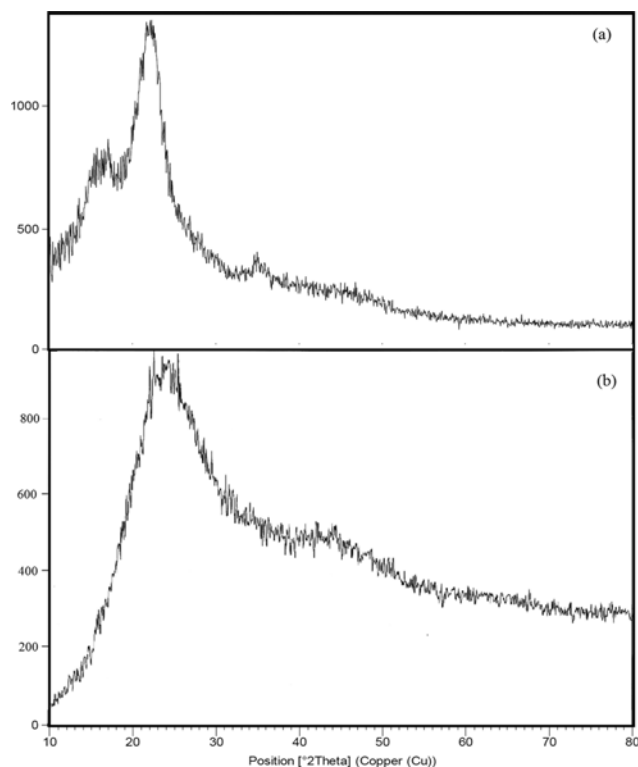


Fig. 4. The XRD patterns of (a) the rice husk sample and (b) the AD-RH sample.

by N_2 adsorption-desorption isotherms are listed in Table 1. Using H_3PO_4 with impregnation ratio 5/1 and 6 min microwave radiation with power 700 W causes the BJH (Barrett-Joyner-Halenda) cumulative surface area of the rice husk to increase from 30.81 to 140.61 m^2/g . The Brunauer-Emmett-Teller surface area of the synthesized adsorbent was obtained as 276.43 m^2/g . The total pore volume was determined as 0.285 cm^3/g and the mean pore diameter is equal to 4.12 nm.

2. Influence of Experimental Parameters on Adsorption

2-1. Effect of Solution Temperature

To determine the effect of temperature on alizarin yellow adsorption, the experiments were performed at four temperatures (25, 30, 35 and 40 $^\circ C$). Adsorption process was performed with adsorbent concentration 0.1 g/L, agitation speed of 200 rpm and initial dye concentration of 10 mg/L for 48 h. The obtained results are shown in Fig. 6, where it can be seen that by increasing temperature from 25 to 40 $^\circ C$, the removal percentage of alizarin yellow decreases from 94% to 84%. So, the removal percentage of dye decreases as temperature increases.

2-2. Effect of Adsorbent Dosage

The effect of adsorbent dosage on the alizarin yellow adsorption is reported in Fig. 7. These experiments were studied over the range 0.1-2 g/L of adsorbent dosages, 50 mL of alizarin yellow with concentration 10 mg/L at pH=6. The results indicate the removal percentage of dye increases to 99.2% by increasing the adsorbent dosage.

3. Adsorption Isotherms

Fitting of equilibrium data with isotherm models helps to obtain the suitable model for dye adsorption process. The obtained data

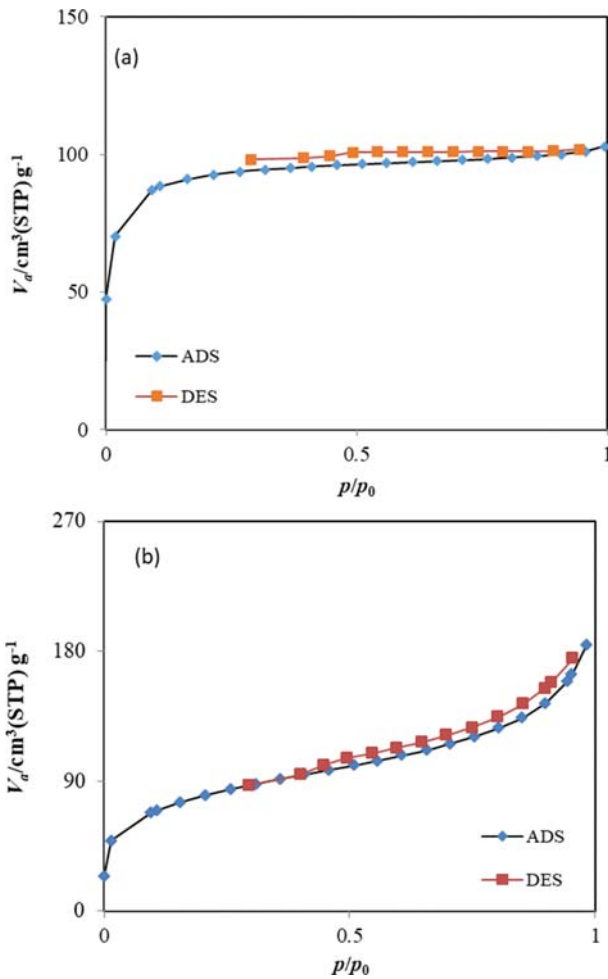


Fig. 5. N₂ adsorption-desorption isotherm of (a) rice husk and (b) AD-RH samples.

Table 1. The surface areas and total pore volumes of the rice husk and AD-RH samples

Parameter	Rice husk	AD-RH
BJH cumulative surface area (m ² /g)	30.81	140.61
Mean pore diameter (nm)	2.68	4.12
BET surface area (m ² /g)	236.83	276.43
Total pore volume (cm ³ /g)	0.159	0.285

from isotherms give some useful information about the capacity and mechanism of adsorption. The equilibrium adsorption data were fitted with Langmuir [22], Freundlich [10], Redlich-Peterson [30], Temkin [39] and Sips [35] isotherms. The equations of these isotherms are:

$$\text{Langmuir isotherm} \quad q_e = \frac{q_m K_L C_e}{1 + K_L C_e} \quad (4)$$

$$\text{Freundlich isotherm} \quad q_e = K_F C_e^{1/n} \quad (5)$$

$$\text{Redlich-Peterson isotherm} \quad q_e = \frac{A C_e}{1 + B C_e^g} \quad (6)$$

$$\text{Temkin isotherm} \quad q_e = B_1 \ln(A_1 C_e) \quad (7)$$

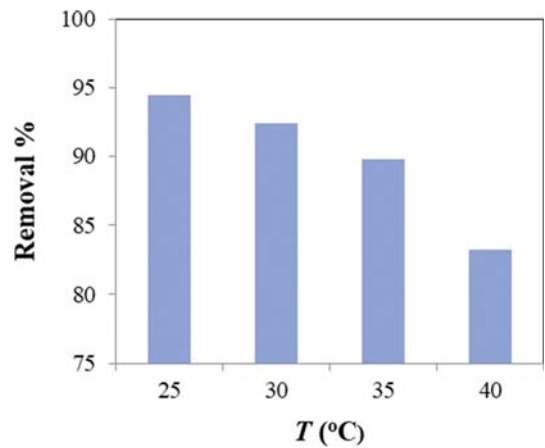


Fig. 6. The effect of temperature on alizarin yellow removal% from aqueous solution (adsorbent dosage=0.1 g/L).

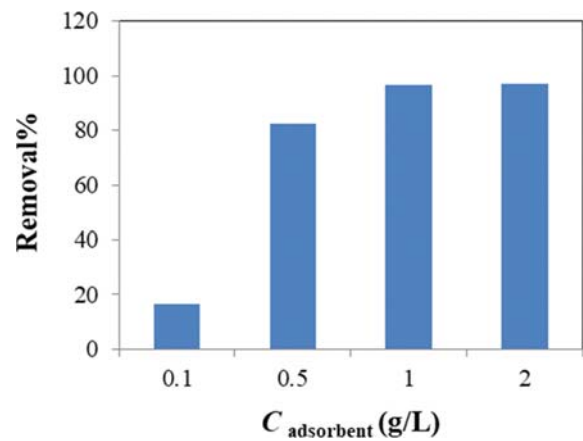


Fig. 7. The effect of adsorbent dosage on alizarin yellow removal% from aqueous solution at 25 °C.

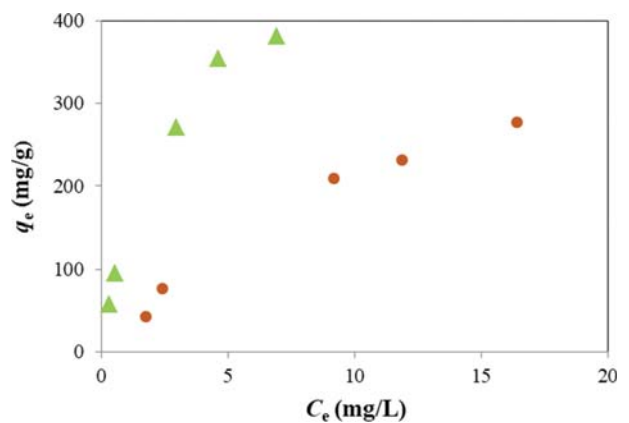


Fig. 8. Adsorption isotherm of alizarin yellow on AD-RH (▲) and CAC (●); at 25 °C and adsorbent dose 0.1 g/L.

$$\text{Sips isotherm} \quad q_e = q_m \frac{(K_{LF} C_e)^{1/n}}{1 + (K_{LF} C_e)^{1/n}} \quad (8)$$

where, K_L , K_F , K_{LF} , A , B , B_T , K_T and g are the constant parameters and q_m is the maximum adsorption capacity; n is a non-dimen-

Table 2. Isothermal parameters of alizarin yellow adsorption on AD-RH and CAC

Models	Parameters	AD-RH	CAC
Langmuir isotherm	q_m (mg/g)	526.31	500.31
	K_L (L/mg)	0.3958	0.7017
	R^2	0.9937	0.7874
Freundlich isotherm	K_f (L/mg)	3.29	34.72
	$1/n$	0.6201	0.7688
	R^2	0.984	0.9328
Redlich-Peterson isotherm	A (L/g)	230.933	31.442
	B (L/mg)	0.49	0.0088
	g (L/mg)	0.7597	1.703
	R^2	0.8206	0.9965
Temkin isotherm	B_T (mg/g)	0.0092	1.0172
	K_T (L/mg)	2.24	24.87
	R^2	0.9907	0.9574
Sips isotherm	q_m (mg/g)	712.633	514.90
	K_{LF} (L/mg)	0.249	0.0600
	$1/n$	0.8639	0.9003
	R^2	0.9999	0.9884

sional parameter relating to surface heterogeneity. Fig. 8 presents the adsorption equilibrium data of AD-RH and CAC. As shown in this figure, the equilibrium amount of adsorbed dye (q_e) on AD-RH is higher than CAC. This result shows that AD-RH can be more effective adsorbent for alizarin yellow removal.

All isotherm equations were fitted with experimental data of

alizarin yellow adsorption on AD-RH and CAC. The results of fittings with the isotherm equations and the values of their correlation coefficients (R^2) are listed in Table 2. The best fitting was obtained by Sips equation. This result shows the adsorption of alizarin yellow on the surface is monolayer and the surface of AD-RH is heterogeneous. The maximum adsorption capacities of AD-RH and CAC (q_m) were obtained 712.63 and 514.90 mg/g, respectively. It is a very high adsorption capacity that was obtained by a low cost adsorbent.

4. Comparison with other Adsorbents

The maximum adsorption capacities of alizarin yellow of various adsorbents are shown in Table 3 [1,11,21,31,43]. In comparison to other adsorbents, including CAC, the low cost adsorbent AD-RH has a high adsorption capacity for alizarin yellow. AD-RH is a nano-adsorbent with an excellent adsorption capacity and thus can be a useful adsorbent.

Table 4 shows some adsorbents which have been prepared by rice husk and their adsorption capacities [8,12,16,23,28,29,45]. It shows microwave radiation with power 700 W for 6 min makes the rice husk an excellent adsorbent with high adsorption capacity. The high adsorption capacity of AD-RH can be due to the electrostatic interactions between surface of AD-RH and negative charge of the anionic dye. This is while the p-p electron donor-acceptor interactions between benzene rings of the dye and the AD-RH surface can be the other possible interactions, leading to high capacity of AD-RH for alizarin yellow adsorption [3].

5. Kinetic Studies

Fig. 9 represents the kinetics of dye adsorption on AD-RH and the CAC at different initial dye concentrations (6, 8 and 10 mg/L). This figure shows the dye adsorption is rapid initially and then it

Table 3. Comparison of adsorption capacities of various adsorbents for alizarin yellow removal

Adsorbent	Adsorption capacity (mg/g)	Activation method	Ref.
Polypyrrole-coated Fe_3O_4 nanoparticles	113.60	Chloride salts of ferrous and ferric ions & ammonium hydroxide & Pyrrole monomers & sodium perchlorate & $FeCl_3$	[11]
Charcoal	14.93	Acid (HCl) and Base (NaOH) treatment	[31]
α -Alumina	18.18	---	[1]
Saccharum spontaneum	13.33	Acid (HCl) treatment	[21]
Ox-MWCNT-PER	45.39	HNO_3 treatment of MWCNTs & modification by PER.	[43]
CAC	514.90	---	This study
AD-RH	712.63	H_3PO_4 & Microwave radiation 700 W	This study

Table 4. Comparison of adsorption capacities of various activated carbons prepared from rice husk

Adsorbate	Heating	Method	Adsorption capacity (mg/g)	Ref.
Malachite green	500 °C	H_3PO_4 & NaOH	80.00	[28]
Cu(II)	750 °C	Pyrolysis & steam	21.10	[45]
Methylene blue	Open air wood fire	NaCl	72.40	[29]
Methylene blue	800 °C	NaOH	396.40	[23]
Paraquat	70 °C	NaOH & Preparation of graft copolymer	317.70	[16]
Safranin-T	110 °C	H_2O_2	74.26	[12]
Methylene blue	500 °C	NaOH & H_2SO_4 & H_3PO_4	543.50	[8]
Alizarin yellow	Microwave radiation 700 W	H_3PO_4	712.63	This study

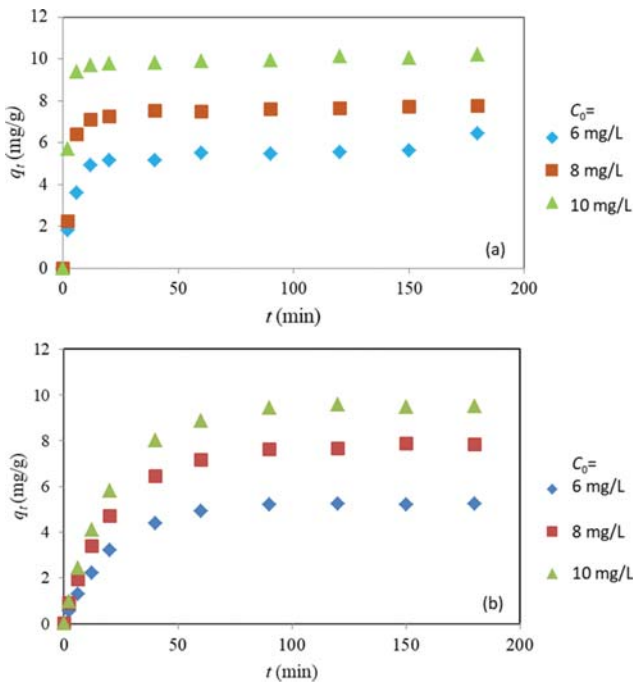


Fig. 9. Adsorption kinetic of alizarin yellow on (a) AD-RH and (b) CAC, ◆: 6 mg/L, ■: 8 mg/L and ▲: 10 mg/L at temperature 25 °C and adsorbent dosage 0.1 g/L.

becomes slower until reaches a constant value at equilibrium time. The fast rate at initial time of adsorption is due to existence of the vacant sites on the surface. Experimental kinetic data show the rate of dye adsorption on AD-RH is faster than CAC.

Pseudo-first-order [20], pseudo-second-order [15], Elovich [44] and Bangham [7] models were applied for fitting of kinetics data.

Pseudo-first-order model $q_t = q_e(1 - \exp(-k_1 t))$ (9)

Pseudo-second-order model $q_t = \frac{q_e k_2 t}{1 + k_2 t}$ ($k_2^* = k_2 q_e$) (10)

Elovich model $q_t = \frac{1}{\beta} \ln(\alpha \beta) + \frac{1}{\beta} \ln t$ (11)

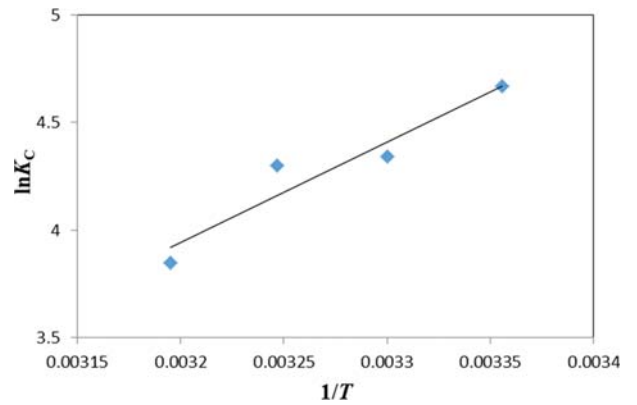


Fig. 10. The diagram of $\ln K_C$ versus $1/T$ of Alizarin yellow adsorption on the synthesized adsorbent.

Bangham model $\ln \ln \left(\frac{C_0}{C_0 - m q_t} \right) = \ln \ln \left(\frac{k_0 m}{2.303 V} \right) + \alpha \ln t$ (12)

where, k_2 and k_1 are the rate constants. β and k_0 are constant and α is the initial adsorption rate. m is adsorbent concentration and V is the solution volume. The kinetic parameters and correlation coefficients, R^2 , were obtained by fitting of kinetic data of dye adsorption on CAC and AD-RH. The results, presented in Table 5, show adsorption of alizarin yellow on AD-RH and CAC obeys pseudo-second-order kinetic model.

6. Thermodynamics Studies

Thermodynamic studies of adsorption have an important role in determining the experiment conditions. The thermodynamic parameter ΔG (kJ/mol) can be computed through the following equations:

$\Delta G = -RT \ln K_C$ (16)

where, T is the solution temperature in Kelvin, K_C is the dimensionless equilibrium constant and R is the gas constant ($8.314 \text{ J mol}^{-1} \text{ K}^{-1}$). K_C was obtained as a dimensionless parameter by multiplying K_L (Langmuir constant) by 55.5 and then 1000 [41]. The other thermodynamic parameters, ΔH (kJ/mol) and ΔS (kJ/mol.K), were obtained by van't Hoff equation:

Table 5. The constants of kinetic models for alizarin yellow adsorption on AD-RH and CAC

Models	Adsorbent	CAC			AD-RH		
	C_0 (mg/L)	6	8	10	6	8	10
Pseudo first order	k_1 (min^{-1})	0.482	0.047	0.457	0.1353	0.0514	0.2145
	R^2	0.9107	0.9937	0.9975	0.9863	0.9746	0.9682
Pseudo second order	k_2 (min^{-1})	0.044	0.0254	0.0438	0.47	0.032	0.054
	R^2	0.9915	0.9956	0.9966	0.9965	0.9984	0.9997
Elovich	α (mg/g.min)	0.8323	1.2525	1.5299	1.8342	4.930	3.8017
	β (g/mg)	0.8476	0.5755	0.4677	0.855	0.953	0.5412
	R^2	0.9612	0.9695	0.9638	0.8234	0.8730	0.8721
Bangham	α	0.7043	0.8222	0.8722	0.9096	0.8147	0.7357
	k_0 (L^2/g)	0.0051	0.0048	0.0044	0.0080	0.0057	0.0137
	R^2	0.9572	0.9927	0.9844	0.9361	0.7943	0.8779

Table 6. The thermodynamic parameters of alizarin yellow adsorption on AD-RH

Temperature	ΔH (kJ/mol)	ΔS (kJ/mol·K)	ΔG (kJ/mol)
298			-11.57
303	-38.87	-0.09	-11.11
308			-10.65
313			-10.20

$$\ln K_C = \frac{-\Delta H}{RT} + \frac{\Delta S}{R} \quad (18)$$

Based on this equation, ΔH and ΔS are determined by the slope and intercept of the plot of $\ln K_C$ against $1/T$. Fig. 10 shows the diagram of the changes $\ln K_C$ versus $1/T$. The results of thermodynamic studies are presented in Table 6. The negative value of ΔG indicates alizarin yellow adsorption on AD-RH is spontaneous. The negative value of ΔH indicates the adsorption process is exothermic. The negative value of ΔS represents a decreasing in randomness due to adsorption, but its amount is very low.

CONCLUSION

Microwave radiation was successfully employed to synthesize a low cost adsorbent (AD-RH) which exhibits an excellent adsorption capacity for alizarin yellow. The microwave radiation on the rice husk was utilized with power 700 W for 6 min. AD-RH is a nano-adsorbent which was used for alizarin yellow removal from aqueous solution. The best condition for dye removal by this adsorbent was obtained at low temperature and high adsorbent dosage. The adsorption capacity of the synthesized adsorbent (712.63 mg/g) shows it is a low cost adsorbent with a high adsorption capacity. Alizarin yellow adsorption on AD-RH and activated carbon of Merck Company was performed by both kinetic and equilibrium point of views. It was shown that AD-RH is a more effective adsorbent for alizarin yellow removal compared with some other adsorbents.

ACKNOWLEDGEMENT

The authors are grateful to University of Kashan for supporting this work by Grant No. (682211/1).

REFERENCES

1. A. A. Azeez, *Tikrit J. Pure Sci.*, **17**, 89 (2012).
2. S. Azizian, M. Haerifar and H. Bashiri, *Chem. Eng. J.*, **146**, 36 (2009).
3. H. Bagheri and A. Mohammadi, *J. Chromatogr. A*, **1015**, 23 (2003).
4. H. Bashiri and S. Nesari, *J. Appl. Chem.*, **14**, 335 (2019).
5. O. Baytar, Ö. Şahin and C. Saka, *Appl. Therm. Eng.*, **138**, 542 (2018).
6. O. Baytar, Ö. Şahin, C. Saka and S. Ağrak, *Anal. Lett.*, **51**, 2205 (2018).
7. S. S. C. Aharoni and E. Hoffer, *J. Chem. Technol. Biotechnol.*, **29**, 404 (1979).
8. Y. Chen, S.-R. Zhai, N. Liu, Y. Song, Q.-D. An and X.-W. Song, *Bioresour. Technol.*, **144**, 401 (2013).
9. S. Eris and H. Bashiri, *Prog. React. Kinet. Mech.*, **41**, 109 (2016).
10. H. Freundlich, *Z. Phys. Chem.*, **57U**, 385 (1907).
11. M. B. Gholivand, Y. Yamini, M. Dayeni, S. Seidi and E. Tahmasebi, *J. Environ. Chem. Eng.*, **3**, 529 (2015).
12. V. K. Gupta, A. Mittal, R. Jain, M. Mathur and S. Sikarwar, *J. Colloid Interface Sci.*, **303**, 80 (2006).
13. B. H. Hameed, J. M. Salman and A. L. Ahmad, *J. Hazard. Mater.*, **163**, 121 (2009).
14. M. Hejazifar, S. Azizian, H. Sarikhani, Q. Li and D. Zhao, *J. Anal. Appl. Pyrolysis*, **92**, 258 (2011).
15. Y.-S. Ho, *J. Hazard. Mater.*, **136**, 681 (2006).
16. S.-T. Hsu and T.-C. Pan, *Bioresour. Technol.*, **98**, 3617 (2007).
17. M. S. İzgi, C. Saka, O. Baytar, G. Saraçoğlu and Ö. Şahin, *Anal. Lett.*, **52**, 772 (2019).
18. Y. Ji, T. Li, L. Zhu, X. Wang and Q. Lin, *Appl. Surf. Sci.*, **254**, 506 (2007).
19. K. M. S. Khalil, O. A. S. Allam, M. Khairy, K. M. H. Mohammed, R. M. Elkhatib and M. A. Hamed, *J. Mol. Liq.*, **247**, 386 (2017).
20. S. Lagergren, *Kungliga Svenska Vetenskapsakademiens Handlingar*, **24**, 1 (1898).
21. A. Lakshmi Narayanan, M. Dhamodaran and J. Samu Solomon, *Int. J. Eng. Appl. Sci.*, **7**, 36 (2015).
22. I. Langmuir, *J. Am. Chem. Soc.*, **38**, 2221 (1916).
23. L. Lin, S.-R. Zhai, Z.-Y. Xiao, Y. Song, Q.-D. An and X.-W. Song, *Bioresour. Technol.*, **136**, 437 (2013).
24. J. A. Menéndez, A. Arenillas, B. Fidalgo, Y. Fernández, L. Zubizarreta, E. G. Calvo and J. M. Bermúdez, *Fuel Process. Technol.*, **91**, 1 (2010).
25. E. Menya, P. W. Olupot, H. Storz, M. Lubwama and Y. Kiros, *Chem. Eng. Res. Des.*, **129**, 271 (2018).
26. L. Muniandy, F. Adam, A. R. Mohamed and E.-P. Ng, *Micropor. Mesopor. Mater.*, **197**, 316 (2014).
27. S. Parra, S. Elena Stanca, I. Guasaquillo and K. Ravindranathan Thampi, *Appl. Catal. B*, **51**, 107 (2004).
28. I. A. Rahman, B. Saad, S. Shaidan and E. S. Sya Rizal, *Bioresour. Technol.*, **96**, 1578 (2005).
29. J. K. Ratan, M. Kaur and B. Adiraju, *Materials Today: Proceedings*, **5**, 3334 (2018).
30. O. Redlich and D. L. Peterson, *J. Phys. Chem.*, **63**, 1024 (1959).
31. M. Salman, M. Athar, U. Shafique, M. Imran, R. Rehman, A. Akram and S. Zulfiqar Ali, *Turkish J. Eng. Env. Sci.*, **35**, 209 (2011).
32. M. Sarabadian, H. Bashiri and S. M. Mousavi, *Clay Miner.*, **1**, in press (2019).
33. M. Sarabadian, H. Bashiri and S. M. Mousavi, *Korean J. Chem. Eng.*, **36**, 1575 (2019).
34. Y. M. Sharif, C. Saka, O. Baytar and Ö. Şahin, *Anal. Lett.*, **51**, 2733 (2018).
35. R. Sips, *J. Chem. Phys.*, **16**, 490 (1948).
36. R. Sivaraj, C. Namasivayam and K. Kadirvelu, *Waste Manage. (Oxford)*, **21**, 105 (2001).
37. N. Soltani, A. Bahrami, M. I. Pech-Canul and L. A. González, *Chem. Eng. J.*, **264**, 899 (2015).
38. S. Somasundaram, K. Sekar, V. K. Gupta and S. Ganesan, *J. Mol. Liq.*, **177**, 416 (2013).
39. M. J. Temkin and V. Pyzhev, *Acta Physicochim. URSS*, **12**, 327 (1940).

40. C. A. Toles, W.E. Marshall, L. H. Wartelle and A. McAloon, *Biore-sour. Technol.*, **75**, 197 (2000).
41. H.N. Tran, S.-J. You and H.-P. Chao, *J. Environ. Chem. Eng.*, **4**, 2671 (2016).
42. M. Uğurlu, A. Gürses and M. Açıkıldız, *Micropor. Mesopor. Mater.*, **111**, 228 (2008).
43. J.-Y. Yang, X.-Y. Jiang, F.-P. Jiao and J.-G. Yu, *Appl. Surf. Sci.*, **436**, 198 (2018).
44. J. Zeldowitsch, *Acta Physicochim. URSS*, **1**, 449 (1934).
45. J. Zhang, H. Fu, X. Lv, J. Tang and X. Xu, *Biomass Bioenergy*, **35**, 464 (2011).
46. Y. Zhou, L. Zhang and Z. Cheng, *J. Mol. Liq.*, **212**, 739 (2015).